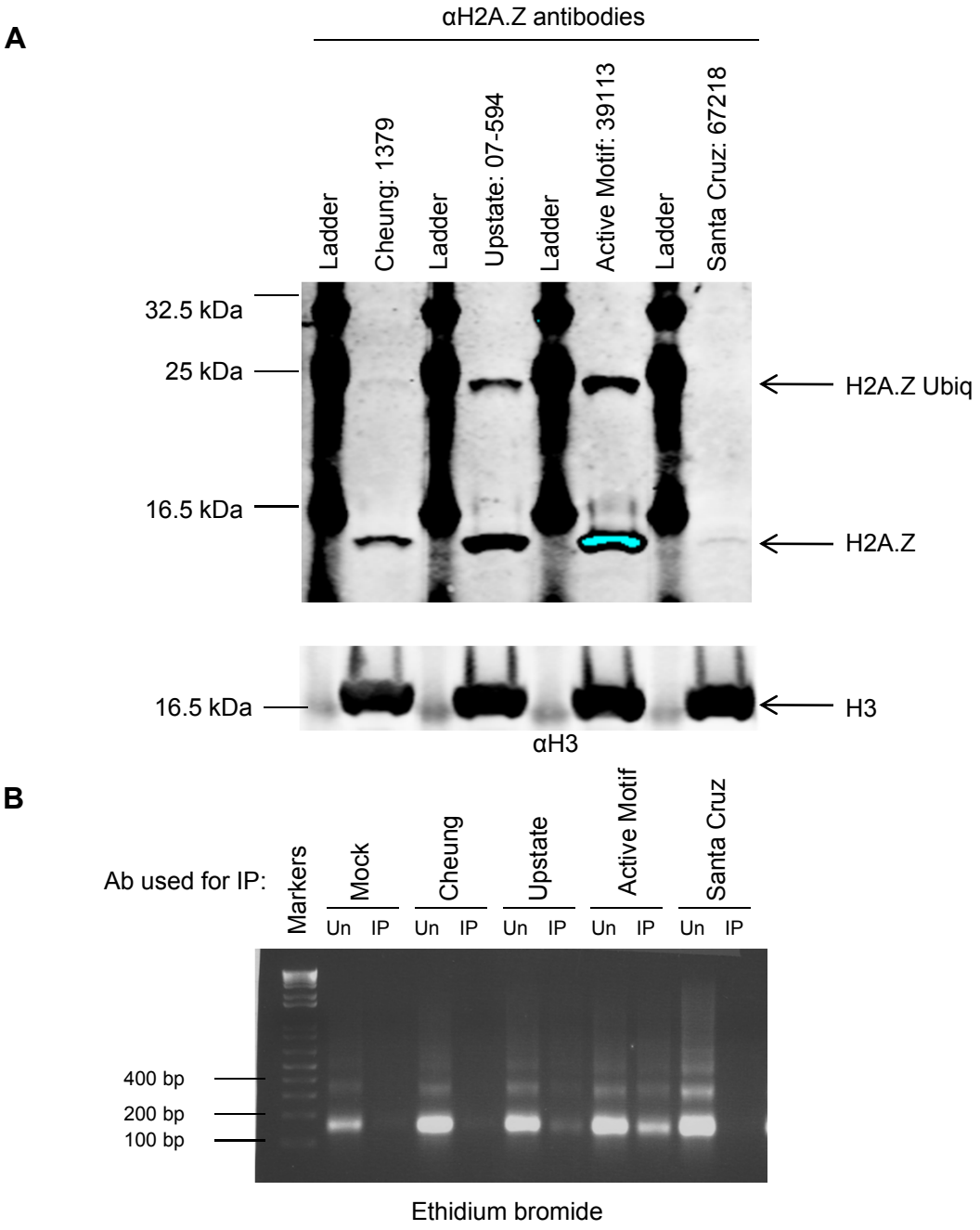

Figure S1. Antibody testing for native H2A.Z ChIPs. We tested antibodies against H2A.Z from P. Cheung (1379), Upstate (07-594), Active Motif (39113), and Santa Cruz (67218) by western anaylsis of total protein *(A)* and DNA recovery *(B)*. *(A)* Nuclear protein from 700,000 cells was loaded into each test lane. The blot was cut into strips and probed with an antibody against total H3 (Abcam 1791) and with the indicated antibody against H2A.Z. Blue indicates saturation. *(B)* Anti-H2A.Z antibodies were tested for performance in our native ChIP assay by electrophoresing DNA from the unbound (Un) and bound (IP) fractions, then comparing the results to a mock ChIP that lacked a primary antibody. Six percent of the unbound and 30% of the IP fractions were run in each lane.

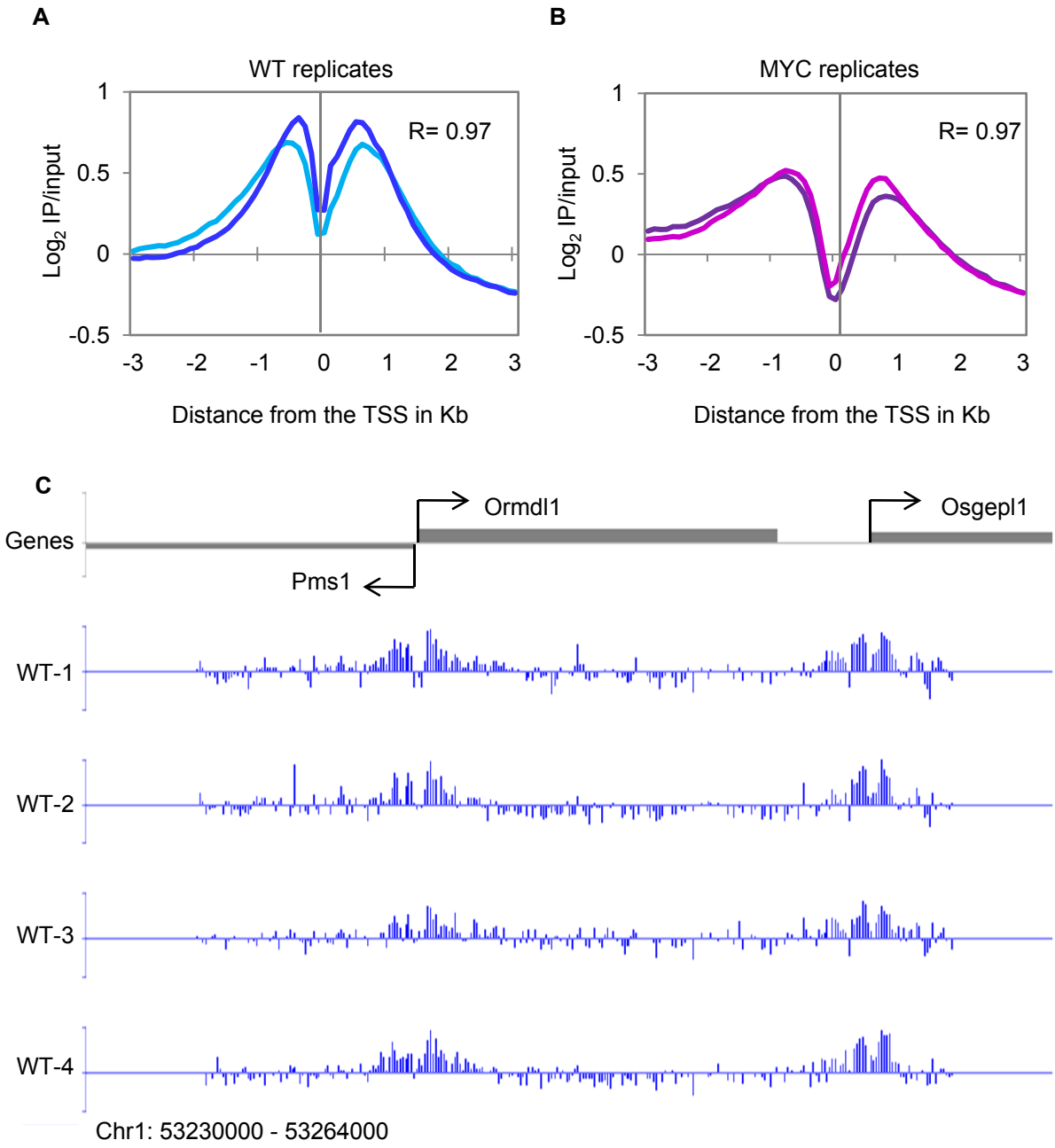

Figure S2. *(A-B)* Average H2A.Z occupancy for all ref-seq genes aligned at the TSS. Two replicates of wild-type (WT) *(A)* and two replicates of MYC *(B)* are shown on the same scale. R values reflect the correlation between the two average occupancy alignments. *(C)* Probes tiled across a random section of the genome for four wild-type (WT) replicates are displayed as the normalized Log_2 of the IP over input. Each vertical bar represents the signal from a single probe.

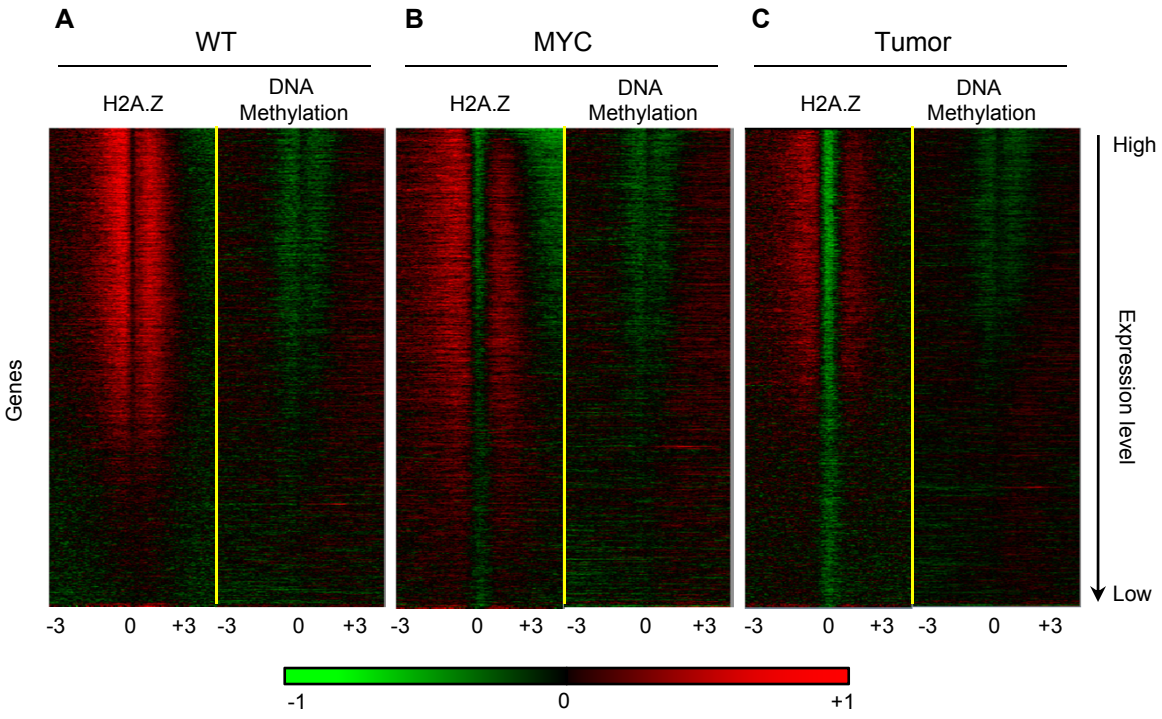

Figure S3. Heat maps of H2A.Z occupancy and DNA methylation for wild-type (WT) *(A),* MYC *(B),* and Lymphoma *(C).* Heat maps are arranged with the highest expressed genes at the top and the lowest expressed genes at the bottom.

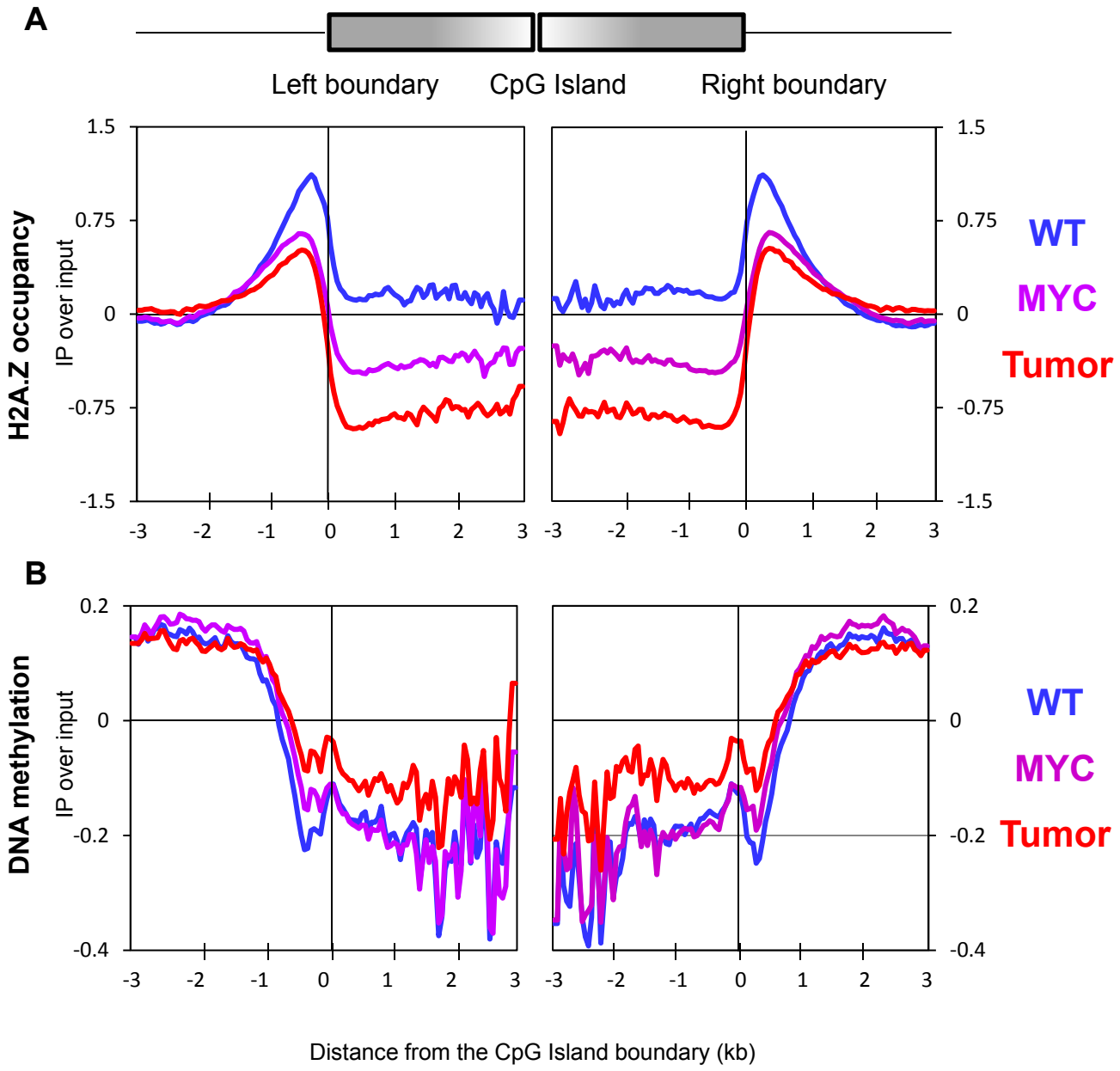

Figure S4. Average H2A.Z occupancy *(A)* and DNA methylation levels *(B)* for all CpG islands aligned at the right and left ends, based on mouse genome annotations available from the UCSC Genome Browser (http://genome.ucsc.edu/). See the legend to Figure 1A-B for details.

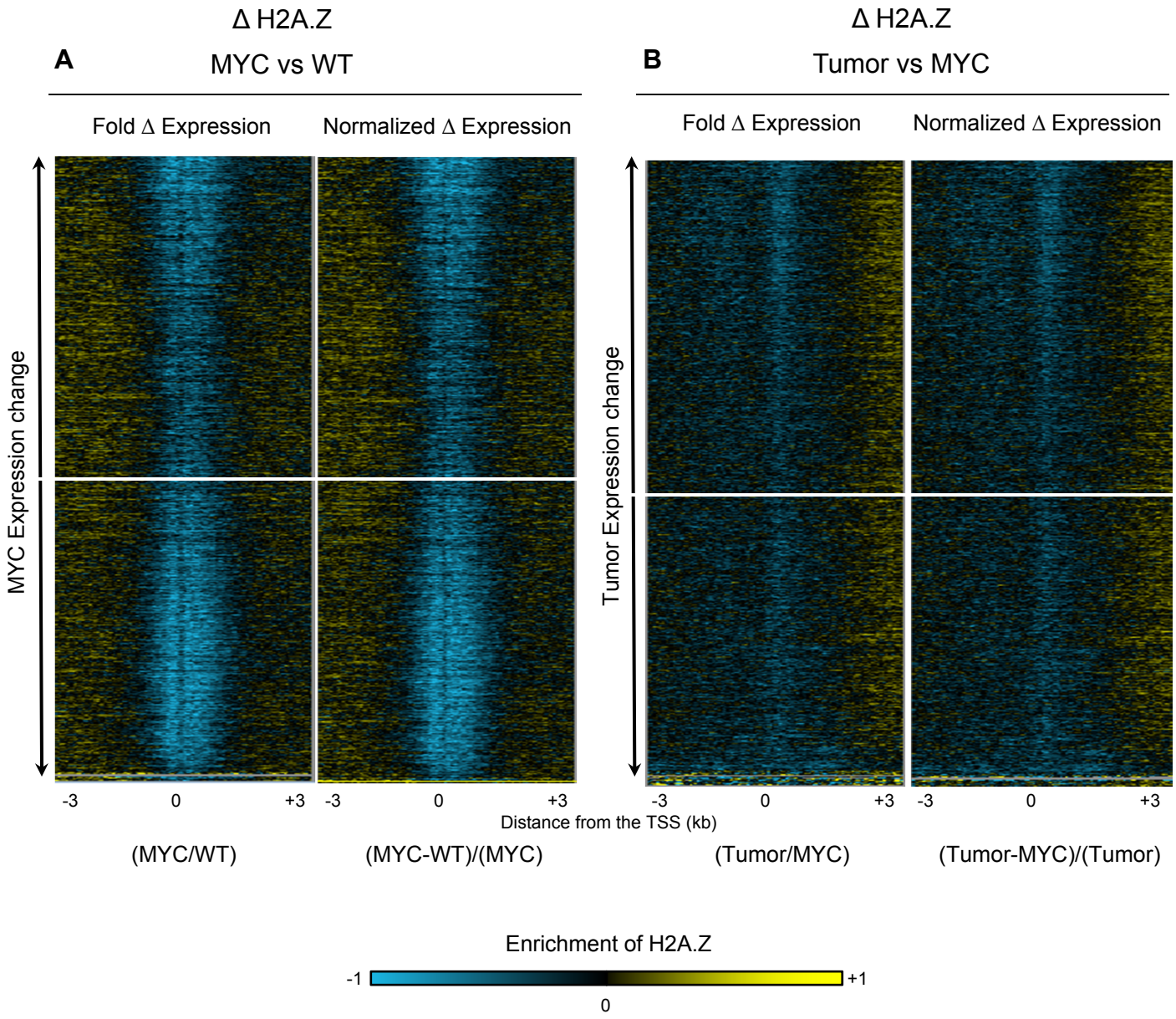

Figure S5. Changes in H2A.Z occupancy from wild-type (WT) to MYC pre-B cells *(A),* and from MYC to lymphoma *(B).* Standard deviate normalized probe signals are represented as heat maps, where yellow indicates an enrichment of ChIP over input signal for H2A.Z and blue represents depletion. *(Left panels)* Genes are ranked by the relative fold change in expression as calculated by (X/Y), where X is the tissue in question and Y is the preceding cell state. *(Right panels)* Genes are ranked by a change in expression as calculated by (X-Y)/X, where X is the tissue in question and Y is the preceding cell state. The genes with the largest gains in expression are at the top, and the genes with the largest decreases in expression level are at the bottom.

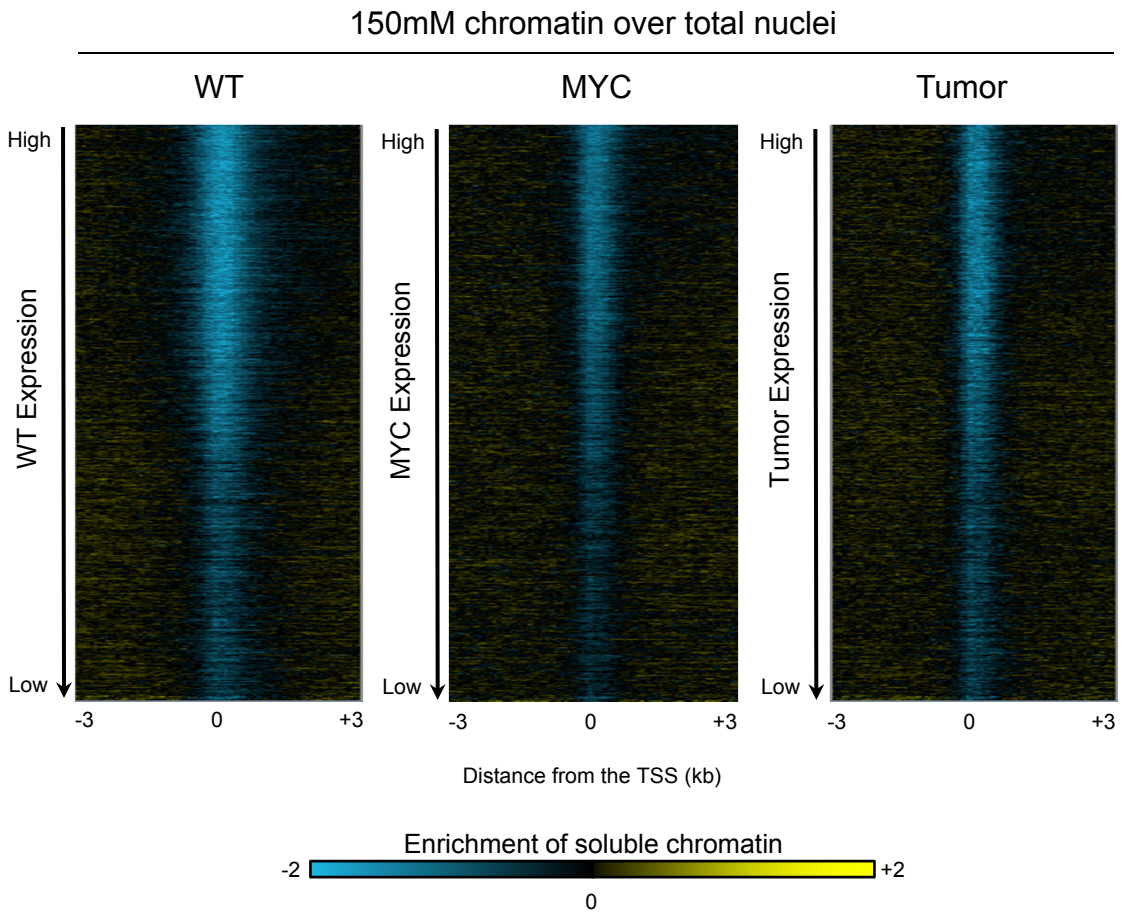

Figure S6. Low salt soluble chromatin (150 mM) over total nuclei for wild-type (WT), MYC, and Tumor. Standard deviate normalized probe signals are represented as heat maps, where yellow indicates an enrichment of soluble chromatin and blue represents depletion. Genes are ranked by expression level, with the most highly expressed genes at the top and the lowest expressed genes at the bottom.

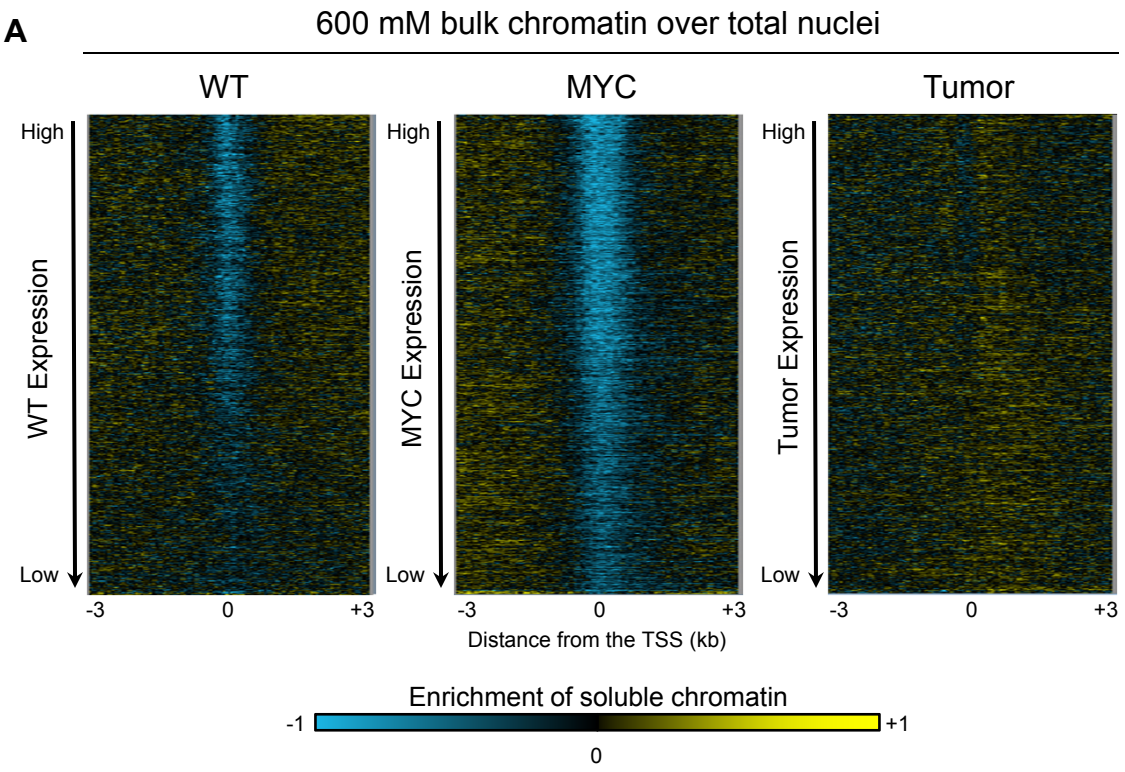

Figure S7. High salt soluble chromatin (600 mM) over total nuclei for wild-type (WT), MYC, and Tumor. Standard deviate normalized probe signals are represented as heat maps, where yellow indicates an enrichment of soluble chromatin and blue represents depletion. Genes are ranked by expression level, with the most highly expressed genes at the top and the lowest expressed genes at the bottom.

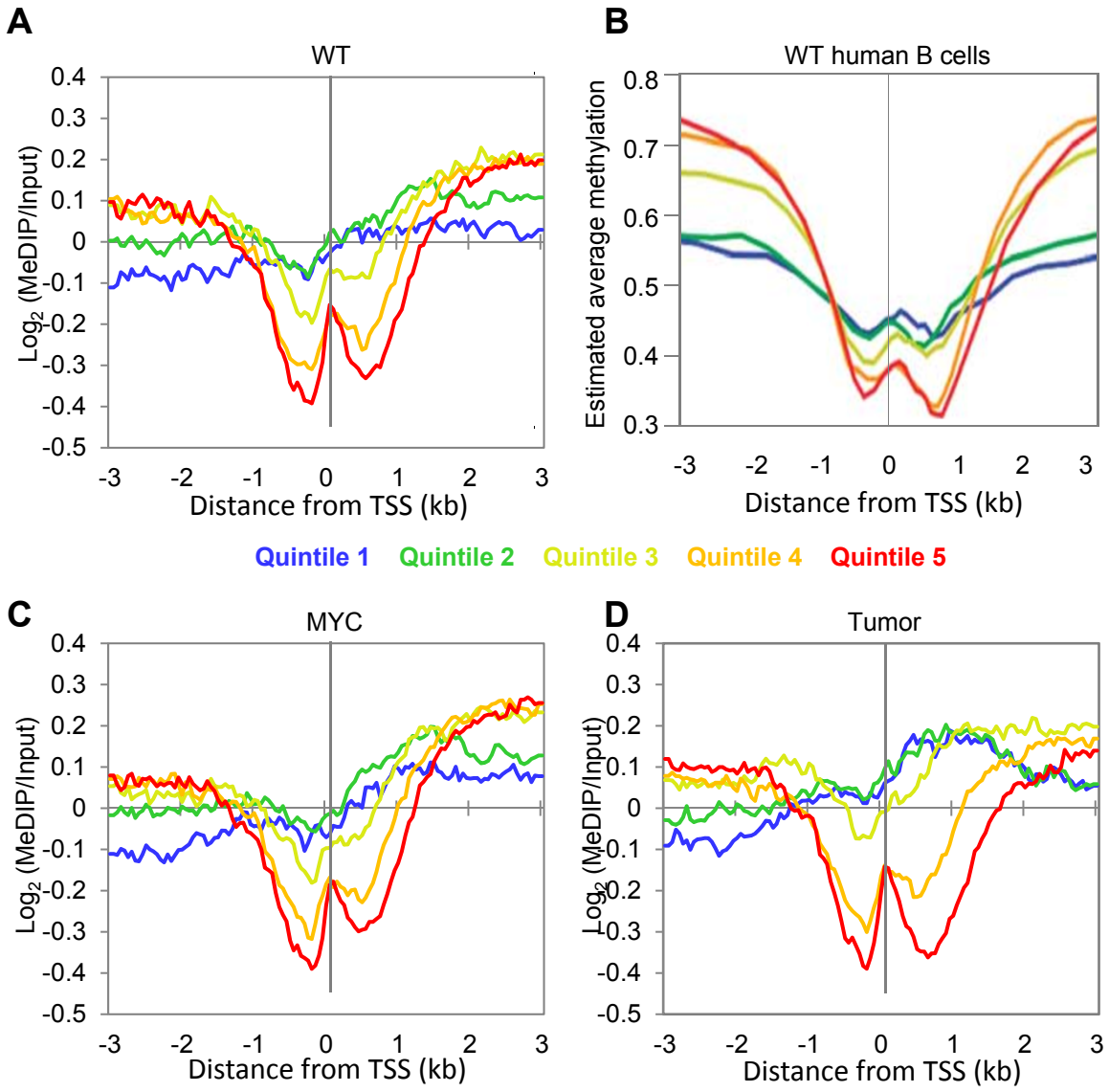

Figure S8. Relationship between DNA methylation around promoters and expression level. Genes were aligned at their TSSs, rank-ordered by expression, and DNA methylation levels were averaged within each quintile of expression. *(A)* Wild-type (WT) mouse pre B-cells. *(B)* For comparison, a similar plot is shown of methylation profiles from wild-type human B cells using a restriction endonuclease-based method with a sequence-based readout, showing average fractions of methylation (reproduced from Ball et al. 2009). *(C)* Eμ-*MYC* pre-B cells. *(D)* Eμ-*MYC* lymphoma cells.

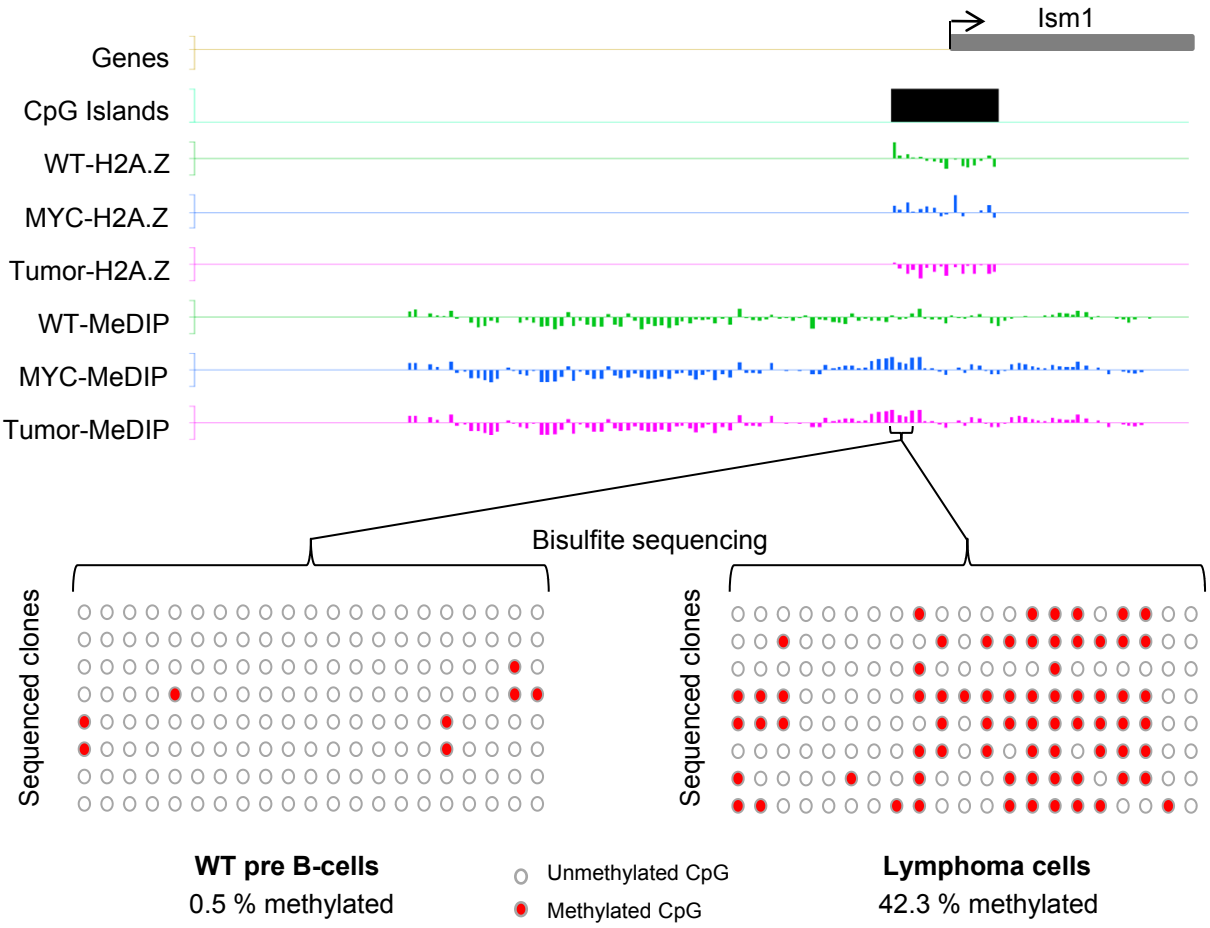

Figure S9. Bisulfite sequence analysis of the Ism1 promoter region. Vertical bars indicate relative log-ratios on the same scale for samples as indicated. Each row of circles represent successive CpGs from a single clone.

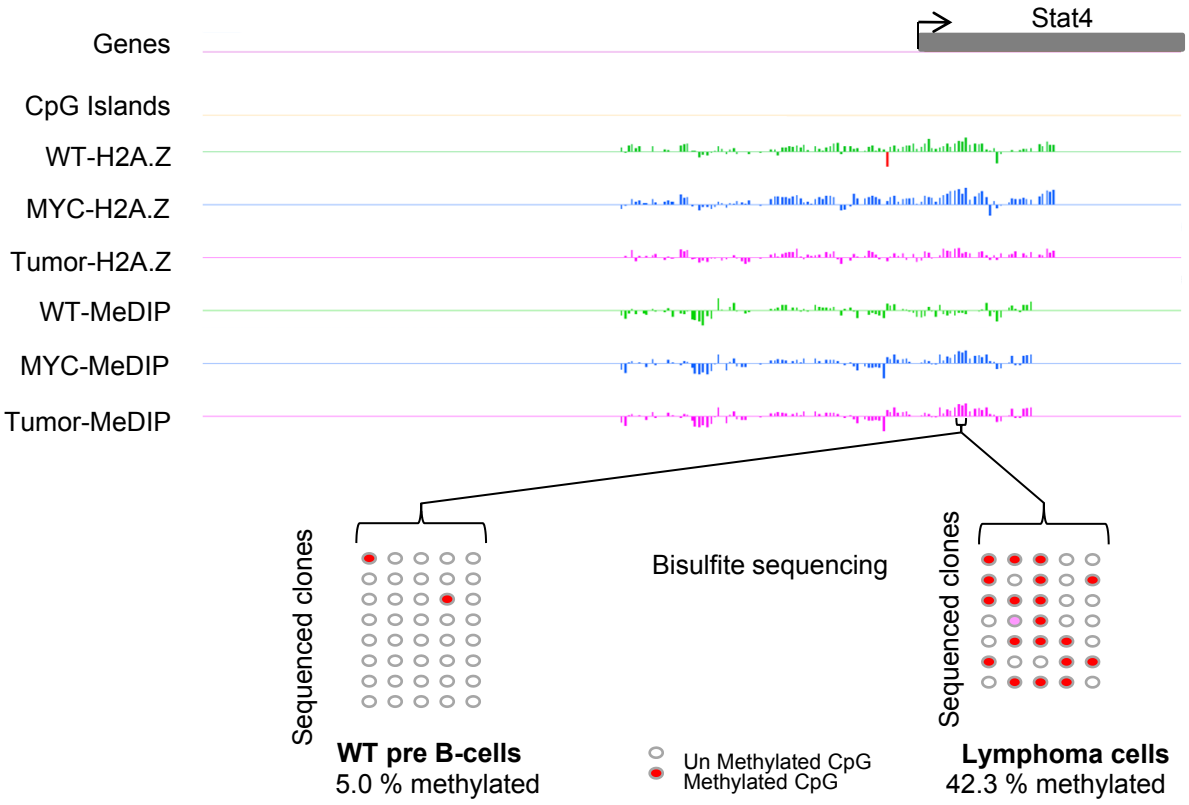

Figure S10. Bisulfite sequence analysis of the Stat4 promoter region. Vertical bars indicate relative log-ratios on the same scale for samples as indicated. Each row of circles represent successive CpGs from a single clone.

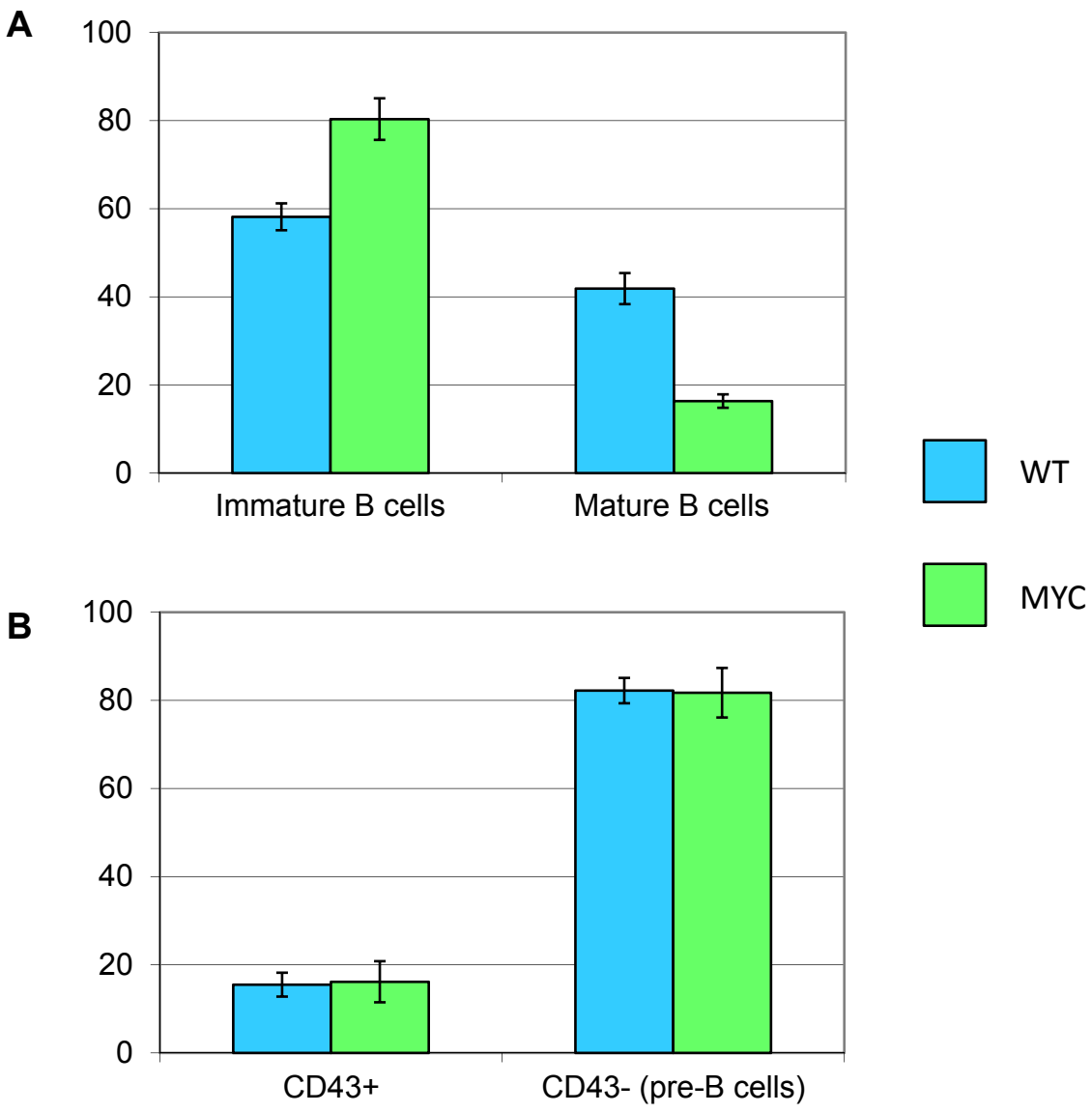

Figure S11. FACS analysis of B220+ cells isolated from the bone marrows of wild-type (WT) and Eμ-*Myc* mice. *(A)* Percentage of immature and mature B cells as assayed by IgM and IgD staining. *(B)* Immature B cells (B200+, IgD- and IgM-) isolated from bone marrows were assayed by staining with cells with CD43 to determine the precentage of pre-B cells (CD43-) in the population. The antibodies used were from eBiosciences: Rat anti-mouse CD45 (RA3-6B2), PE rat anti-mouse CD43 (S7) PE-Cy7 anti-mouse IgM (II/41), FITC anti-mouse IgD (11-26). Reference: Hardy, R. and Shinton, S. Characterization of B lymphogenesis in mouse bone marrow and spleen. In Methods in Molecular biology, v. 271, 2004 (Humana Press).

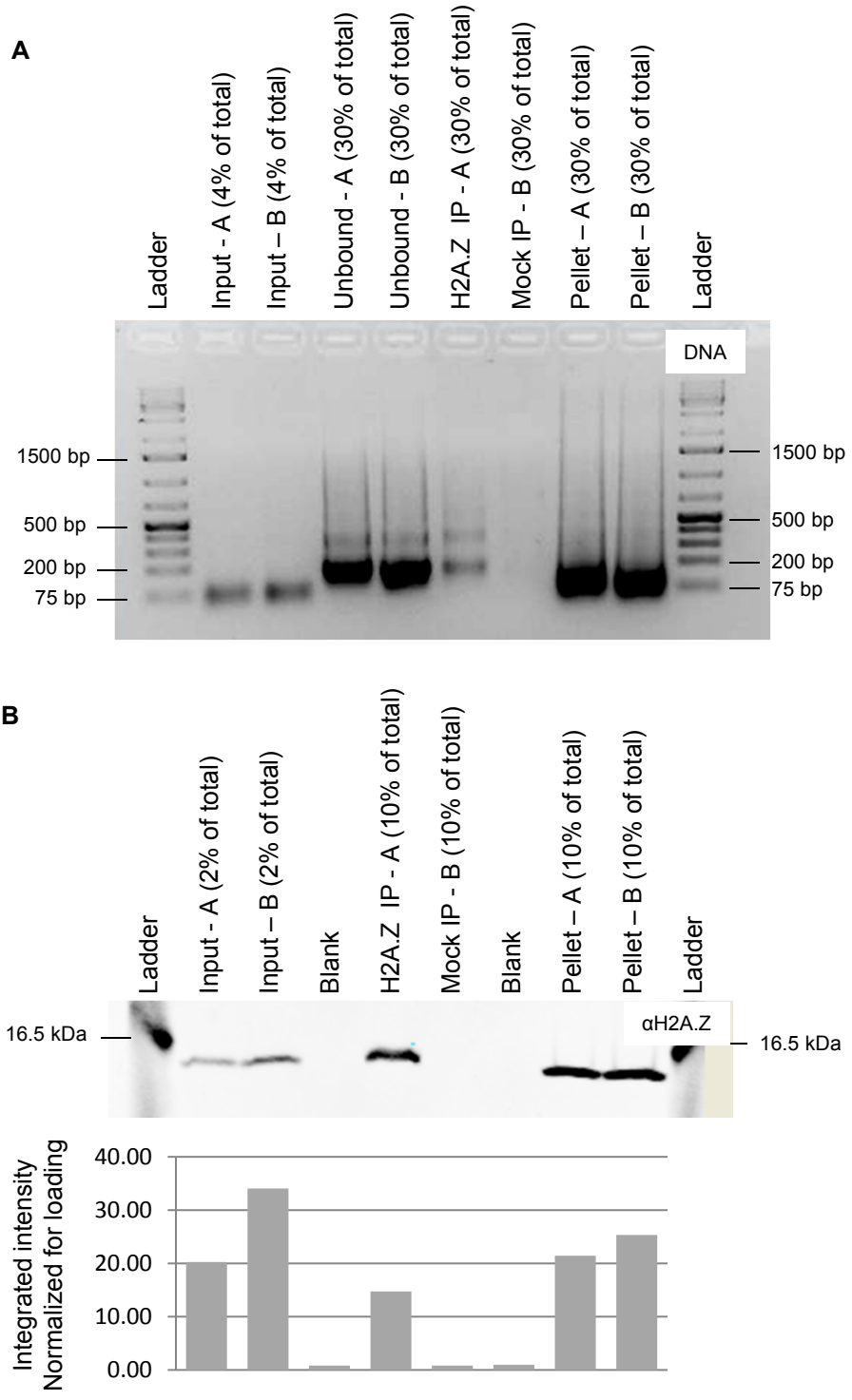

Figure S12. *(A)* DNA fractions from native H2A.Z and mock IPs. The percentage of the fraction loaded on the gel is listed above each lane. *(B)* Western blot for H2A.Z of fractions from H2A.Z and mock IPs. The percentage of the fraction loaded on the gel is listed above each lane. Below each lane on the blot, the signal from the IRD labeled secondary is shown, normalized for the percentage of protein loaded. The H2A.Z in the IP fraction tends to run slightly higher, probably due to the increased salt concentration as all the histones in the IP fraction run slightly high.